Optineurin regulates osteoblastogenesis through STAT1

Noriyoshi Mizuno[a*], Tomoyuki Iwata[a], Ryosuke Ohsawa[b], Kazuhisa Ouhara[a], Shinji Matsuda[a], Mikihito Kajiya[a], Yukiko Matsuda[b], Kodai Kume[b], Yui Tada[b], Hiroyuki Morino[b], Tetsuya Yoshimoto[c], Yasuyoshi Ueki[c], Keichiro Mihara[d], Yusuke Sotomaru[e], Katsuhiro Takeda[f], Syuichi Munenaga[g], Tsuyoshi Fujita[a], Hiroyuki Kawaguchi[g], Hideki Shiba[f], Hideshi Kawakami[b], Hidemi Kurihara[a]

[a]Department of Periodontal Medicine, Graduate School of Biomedical and Health Sciences, Hiroshima University, 1-2-3, Kasumi, Minami-ku, Hiroshima, 734-8553, Japan

[b]Department of Epidemiology, Research Institute for Radiation Biology and Medicine, Hiroshima University, Hiroshima, 1-2-3, Kasumi, Minami-ku, Hiroshima, 734-8553, Japan

[c]Department of Biomedical Sciences and Comprehensive Care, Indiana University School of Dentistry, 635 Barnhill Drive, Indianapolis, IN 46202, USA

[d]International Regenerative Medical Center, Fujita Health University, 1-98 Dengakugakubo, Kutsukake-cho, Toyoake, Aichi, 470-1192, Japan

[e]Natural Science Center for Basic Research and Development, Hiroshima University, Hiroshima, 1-2-3, Kasumi, Minami-ku, Hiroshima, 734-8553, Japan

[f]Department of Biological Endodontics, Graduate School of Biomedical and Health Sciences, Hiroshima University, 1-2-3, Kasumi, Minami-ku, Hiroshima, 734-8553, Japan

---

This is the author's manuscript of the article published in final edited form as:

Mizuno, N., Iwata, T., Ohsawa, R., Ouhara, K., Matsuda, S., Kajiya, M., Matsuda, Y., Kume, K., Tada, Y., Morino, H., Yoshimoto, T., Ueki, Y., Mihara, K., Sotomaru, Y., Takeda, K., Munenaga, S., Fujita, T., Kawaguchi, H., Shiba, H., … Kurihara, H. (2020). Optineurin regulates osteoblastogenesis through STAT1. Biochemical and Biophysical Research Communications, 525(4), 889–894. https://doi.org/10.1016/j.bbrc.2020.03.028

[g]Department of General Dentistry, Hiroshima University Hospital, 1-2-3, Kasumi, Minami-ku, Hiroshima, 734-8553, Japan

[*]**Corresponding authors**

Noriyoshi Mizuno, DDS, PhD

1-2-3 Kasumi, Minami-ku, Hiroshima, 734-8553 Japan

Tel: +81-82-257-5663

Fax: +81-82-257-5664

Email: mizuno@hiroshima-u.ac.jp

ABSTRACT

A sophisticated and delicate balance between bone resorption by osteoclasts and bone formation by osteoblasts regulates bone metabolism. *Optineurin (OPTN)* is a gene involved in primary open-angle glaucoma and amyotrophic lateral sclerosis. Although its function has been widely studied in ophthalmology and neurology, recent reports have shown its possible involvement in bone metabolism through negative regulation of osteoclast differentiation. However, little is known about the role of OPTN in osteoblast function. Here, we demonstrated that OPTN controls not only osteoclast but also osteoblast differentiation. Different parameters involved in osteoblastogenesis and osteoclastogenesis were assessed in $Optn^{-/-}$ mice. The results showed that osteoblasts from $Optn^{-/-}$ mice had impaired alkaline phosphatase activity, defective mineralized nodules, and inability to support osteoclast differentiation. Moreover, OPTN could bind to signal transducer and activator of transcription 1 (STAT1) and regulate runt-related transcription factor 2 (RUNX2) nuclear localization by modulating STAT1 levels in osteoblasts. These data suggest that OPTN is involved in bone metabolism not only by regulating osteoclast function but also by regulating osteoblast function by mediating RUNX2 nuclear translocation via STAT1.

Keywords: OPTN, Osteoclast, Osteoblast, STAT1, RUNX2

1. Introduction

Optineurin (OPTN) is a gene linked to primary open-angle glaucoma (POAG) and (ALS) [1,2]. POAG is characterized by progressive neurodegeneration of retinal ganglion cells. The E50K OPTN mutation was first identified in familial POAG [1]. Transgenic mice models showed that E50K OPTN induces the apoptosis of retinal ganglion cells and progressive retinal degeneration exclusively [3]. On the other hand, ALS is a devastating disorder characterized by progressive degeneration of motor neurons of the primary motor cortex, brainstem, and spinal cord. Three types of mutations of OPTN in ALS patients were reported, such as homozygous deletion of exon 5, a homozygous Q398X nonsense mutation, and a heterozygous E478G missense mutation within its ubiquitin-binding domain [2]. OPTN is involved in basic cellular functions, including protein trafficking, maintenance of the Golgi apparatus, and the NF-κB pathway [2,4]. The NF-κB pathway is an important signal transduction pathway regulating immune response and inflammation. OPTN exhibits the high sequence homology to NF-κB essential modulator (NEMO) and suppresses NF-κB activity by competing with NEMO [5,6]. Cell transfection experiments showed that wild type (WT) OPTN and E50K mutant inhibit NF-κB activity, but ALS-related OPTN mutants were unable to inhibit NF-κB activity in cultured cells [2,7]. Furthermore, the ALS-related OPTN missense mutation revealed a cytoplasmic distribution different from that of WT [2]. Therefore, OPTN is

thought to be involved in a significant part of the pathogenesis of ALS. Therefore, E50K and ALS-related OPTN mutants are thought to be involved in different intracellular signaling.

Recently, linkage studies have revealed a strong susceptibility for Paget's disease of bone (PDB) in the *OPTN* locus [8,9]. PDB is a skeletal disease characterized by excess osteoclasts activation, which causes increased but disorganized bone turnover. The most known responsible gene is *sequestosome 1 (p62)*, which is mutated in more than 10% of patients [10,11]. Recent studies have revealed that homozygous loss-of-function mutations (D477N) in *OPTN* enhance osteoclasts activity and predispose to PDB [12]. Moreover, OPTN is suggested to have an inhibitory effect on NF-κB as well as the IFN-B signaling pathway [13,14]. Bone metabolism is regulated by osteoblasts and osteoclasts cooperatively, and these activities are coupled inextricably [15]. To date, various molecules, including SH3BP2, Semaphorin 3A, and Bcl6, have been shown to regulate both osteoblasts and osteoclasts and could serve as potential strategies for the treatment of bone loss in inflammatory bone disease [16-19]. However, little is known about the precise role of OPTN in bone metabolism. In this study, we investigated the potential role of OPTN in regulating osteoblast differentiation using $Optn^{-/-}$ mice.

2. Materials and methods

2.1. Mice

Optn$^{-/-}$ mice with a C57BL/6 background generated in a previous study [*Optn*-exon 8 deletion, Kurashige et al. in preparation] were used. The Mice were kept in a specific pathogen-free room with a 12 h light-dark cycle at a constant temperature. All procedures for animal uses were approved by the Committee of Research Facilities for Laboratory Animal Science, Hiroshima University School of Medicine.

2.2. Reagents and antibodies

Antibodies for immunohistochemistry, immunoprecipitation, western blotting, and immunofluorescent staining were obtained from Cell Signaling Technology (CST) (Danvers, MA, USA), Santa Cruz Biotechnology (Santa Cruz, CA, USA), GeneTex (Irvin, CA, USA), Abcam (Cambridge, MA, USA) and Cayman Chemical (Ann Arbor, MI, USA).

2.3. Histomorphometric Analysis of Bone

Femora were fixed in 70% ethanol and embedded in glycolmethacrylate without decalcification. Serial sections were cut and stained with Villanueva bone stain. Part of the histomorphometric analysis was performed at the Ito Bone Science Institute (Niigata, Japan).

2.4. Immunohistochemistry

Paraffin-embedded femora were sectioned (3 μm) and rehydrated. Endogenous horseradish peroxidase was blocked with 3% hydrogen peroxide in phosphate-buffered saline (PBS) after deparaffinization. After blocking with normal horse serum, the sections were incubated overnight at 4°C with an anti-RUNX2 antibody (M-70, Santa Cruz Biotechnology). After washing three times with PBS, sections were incubated with biotinylated anti-rabbit or goat IgG antibody for 30 min at room temperature. After washing with PBS, the sections were reacted with CSA II, Biotin-Free Catalyzed Amplification System, (DAKO, Carpinteria, CA, USA) for 30 min. The immunohistochemical analysis was performed at the Kureha Special Laboratory (Fukushima, Japan).

2.5. Osteoblasts culture and bone nodule assay

Osteoblasts were isolated from the calvarial bones of 2–days-old mice by collagenase/dispase digestion. Cells were cultured on 12 well plates at a density of 1×10^5 cells/well. Osteoblast differentiation was induced by osteogenic medium (α -minimal essential medium (α-MEM) (Sigma-Aldrich, St. Louis, MO, USA) supplemented with 10% fetal bovine serum (FBS) (Thermo Scientific, Waltham, MA, USA), 10 mM β-glycerophosphate, 10^{-8} M dexamethasone, and 100 μg/ml ascorbic acid). The cells were cultured for 21 days, and the culture medium was changed every 2 days. Subsequently, the alkaline phosphatase (ALP) activity was assessed, and the mineralized

nodules were detected using alizarin red staining. For ALP activity assessment the osteoblasts were stained using p-nitrophenylphosphate after 7, 14, or 21 days of culture. Subsequently, the osteoblasts were lysed with 0.025 % Triton X solution followed by centrifugation at 15,000 rpm for 15 min. The ALP activity was measured in the supernatant using a Lab Assay ALP kit (Wako, JAPAN). The absorbance of the resultant solution was measured at 405 nm.

2.6. Immunoprecipitation

Immunoprecipitation was performed using Dynabeads® Protein G (Invitrogen, Carlsbad, CA, USA) according to the manufacturer's protocols. After being cultured in osteogenic medium for 3 days, cell lysates were isolated by RIPA buffer and incubated for 3 h with a Dynabeads-anti-STAT1 antibody (Abcam) at room temperature. The lysate/antibody/bead complex was washed extensively with PBS-Tween (0.1%). The proteins captured by the anti-STAT1 antibody-coated beads were subsequently separated using SDS-PAGE and subjected to western blotting with a rabbit anti-mouse STAT1 antibody (CST) and rabbit anti-mouse OPTN antibody (Cayman).

2.7. Western blotting

Protein samples were subjected to electrophoresis on a 10% SDS-polyacrylamide gel and transferred to a nitrocellulose membrane (Bio-Rad Laboratories, Hercules, CA, USA). After being blocked for 1 h (5% nonfat milk in TBS plus 0.1% Tween 20), the membrane was incubated at 4°C

overnight with rabbit anti-mouse STAT1 (CST) and rabbit anti-mouse β-actin (CST). The membrane was washed thrice and incubated with HRP-conjugated secondary goat anti-rabbit antibodies (R&D Systems, Minneapolis, MN, USA) at room temperature for 1 h. Immunodetection was performed according to the protocols supplied with ECL Prime Western blotting detection reagents (BioRad Laboratories, Hercules, CA, USA).

2.8. Immunofluorescent staining

Osteoblasts cultured in osteogenic medium (2.0×10^5 cells/well in 24-well chamber slides) were fixed in 4% paraformaldehyde (PFA), permeabilized with 0.1% Triton X-100, and blocked in 1% bovine serum albumin. These slides were incubated with anti-RUNX2 antibody (Santa Cruz Biotechnology) at 4°C overnight. RUNX2 was detected by Alexa Fluor-488 goat anti-mouse IgG antibody. Nuclei were stained with 4, 6-diamidino-2-phenylindole (DAPI). Fluorescence signals were detected with the use of the Zeiss LSM 510 laser scanning confocal microscope (Zeiss Microimaging, LCM, Zeiss Jena, Germany). Cells were considered positive for RUNX2 nuclear localization when the fluorescence intensity of RUNX2 in nuclei exceeded that in the cytoplasm. Numbers of DAPI-positive and RUNX2 positive nuclei were counted, and the percentages of RUNX2 positive nuclei per total nuclei were calculated.

2.9. Osteoblast-osteoclast co-culture assay

Osteoblasts (at a density of 5×10^4 cells/well) were co-cultured with BMCs (at a density of 5×10^5 cells/well) in a 24-well plate in α-MEM with 10% FBS, 10 nM $1\alpha,25(OH)_2D3$ and penicillin/streptomycin. The culture medium was changed every 2 days, and the cells were fixed after 8 days. TRAP-positive MNCs were counted.

2.10. Real-time polymerase chain reaction (PCR)

Total RNA was extracted using RNAiso Plus (TAKARA, JAPAN). cDNA was synthesized using ReverTraAce (TOYOBO, JAPAN). Real-time PCR was done using a Syber Green.

2.11. Statistical analysis

The results were expressed as mean ± standard deviations (SD). Statistical differences between the mean values of control and experimental groups were analyzed by using Student's t-test at a significance level of 1% or 5%.

3. Results

3.1. OPTN regulates bone formation *in vivo*

The immunohistochemical analysis to study the bone morphology revealed nonsignificant differences for osteoblasts surfaces per bone surface (Obs/BS) and osteoblasts number per bone surface (ObN/BS) between $Optn^{-/-}$ and WT mice (Fig. 1A-C). Histomorphometric analysis, calcein,

and tetracycline labeling showed that mineral apposition rate (MAR) and bone formation rate per bone surface (BFR/BS) were lower in Optn$^{-/-}$ mice (Fig. 1D-G). Osteoid thickness (Oth), Osteoid maturation time (Omt), and Mineralization lag time (Mit) were higher in Optn$^{-/-}$ mice (Fig. 1H-J). The observations showing significantly lower bone formation in Optn$^{-/-}$ mice indicated the potential role of OPTN in the regulation of bone formation.

3.2. OPTN promotes osteoblast differentiation through STAT1 inhibition

To reveal whether OPTN affects osteoblast differentiation and function *in vitro*, we quantified the ALP activity and assessed the mineralized nodule formation by alizarin red staining. The results revealed a reduced ALP staining as well as ALP activity in the osteoblasts from Optn$^{-/-}$ mice as compared with the WT mice (Fig. 2A, B). Mineralized nodules stained by alizarin red in osteoblasts from Optn$^{-/-}$ mice were also reduced (Fig. 2C, D). These data indicated that OPTN is required for the differentiation of osteoblasts.

Furthermore, to elucidate the molecular mechanism of OPTN on osteoblast differentiation, the OPTN target candidates were explored by searching for the proteins that bind to OPTN, and the screening molecules that regulate osteoblast differentiation. Based on these criteria, we identified STAT1 that has been reported to regulate osteoblast differentiation negatively. The immunoprecipitation analysis revealed that OPTN binds to STAT1 (Fig. 3A), and the expression

level of STAT1 protein in Optn$^{-/-}$ osteoblasts was significantly higher than that in WT osteoblasts (Fig. 3B). These results suggested that OPTN could have directly suppressed STAT1 in osteoblasts. Moreover, STAT1 is reported to suppress osteoblast differentiation by inhibiting the nuclear translocation of RUNX2. Therefore, we investigated whether RUNX2 translocation into the nucleus was inhibited in Optn$^{-/-}$ mice. Immunofluorescent staining showed that nuclear translocation of RUNX2 by osteoblastic induction was significantly inhibited in Optn$^{-/-}$ osteoblasts (Fig. 3C) and that the percentages of RUNX2 positive nuclei were smaller in Optn$^{-/-}$ osteoblasts (Fig. 3D).

3.3. The ability to support osteoclast differentiation is reduced in osteoblasts from Optn$^{-/-}$ mice

The osteoblast-osteoclast co-culture assay revealed that the osteoblasts from Optn$^{-/-}$ mice had reduced ability to support osteoclast differentiation compared to those from WT mice, as evident from the reduced level of TRAP-positive MNCs in Optn$^{-/-}$ mice (Fig. 4A). Expression of *Tnfsf11* mRNA in osteoblast cultures from Optn$^{-/-}$ mice was significantly lower than that from WT mice (Fig. 4B).

4. Discussion

We identified OPTN as an important regulator of bone metabolism that regulates osteoblast differentiation and function. We analyzed different parameters involved in osteoblastogenesis and osteoclastogenesis. Analysis of bone morphology revealed nonsignificant differences for Obs/BS

and ObN/BS; however, we observed an increased osteoid thickness in Optn$^{-/-}$ mice, which could be due to a functional defect of osteoblast. Comparison of dynamic bone formation indices revealed a significant decrease in BFR/BS, MAR, and other mineralization related parameters, suggesting the role of OPTN in mineralization defect *in vivo*. Here, we assessed ALP activity by alizarin red staining to study osteoblast activity. Generally, ALP is considered to be an early marker of osteoblast differentiation, and an increased level of ALP refers to active bone formation [20]. In the present study, the reduced ALP activity in Optn$^{-/-}$ mice indicated that OPTN is required for the differentiation of osteoblasts. Furthermore, we have assessed the mineralization of bone cells by alizarin red staining. Alizarin red staining is one of the most common methods used to examine a mineralized matrix [21, 22]. It allows simultaneous evaluation of mineral distribution and inspection of small structures and is particularly versatile in that the dye can be extracted from the stained monolayer and readily quantified [20]. In this study, alizarin red mineralization was found to be reduced in Optn$^{-/-}$ mice, indicating impaired osteoblastogenesis in the absence of OPTN.

STAT1 inhibits osteoblast differentiation by inhibiting RUNX2 transcriptional activity and RUNX2 nuclear translocation, which has been reported to have a key role in osteogenic differentiation and bone formation [23]. In the present study, the immunoprecipitation analysis revealed that STAT1 binds to OPTN and the RUNX2 localization in nuclei was significantly inhibited in Optn$^{-/-}$ osteoblasts.

In this study, we have found that OPTN is also able to inhibit osteoclast differentiation *in vitro* as it attenuates the formation of TRAP-positive MNCs. *TNFSF11* gene can stimulate osteoclast formation and is a critical mediator of bone resorption and overall bone density. Here, the real-time PCR analysis of *tnfsf11* mRNA expression analysis revealed dysfunctional osteoclasts in $Optn^{-/-}$ mice as compared to WT mice. Collectively, the results of the present study revealed the importance of OPTN in bone remodeling.

However, Obaid et al. [12] have identified OPTN as a negative regulator of osteoclast differentiation using a mouse model of PDB ($Optn^{D477N/D477N}$ mice). They have suggested that the common genetic variant rs1561570 (D477N) at the OPTN locus increases susceptibility to PDB by reducing levels of OPTN expression, leading to enhanced osteoclast differentiation. Although the study reported the detailed analysis of bone phenotype in $Optn^{D477N\ /\ D477N}$ mice, the inhibition of OPTN expression level has not been thoroughly explored. In addition, since bone metabolism is explained by the delicate relationship between osteoblasts and osteoclasts, it may differ in different mice models, thus creating a discrepancy between the two studies. Moreover, OPTN signaling is a complicated process involving many molecules, such as CYLD, TANK-binding kinase I, IKKε, caspase 8, and STAT1 [5,13,14,24]. In addition, other signaling factors may have existed concerning osteoblast differentiation in OPTN signaling. So, further detailed analysis of the bone phenotypes in $Optn^{-/-}$ mice is necessary in the future.

In summary, OPTN controls not only osteoclast but also osteoblast differentiation in bone metabolism. We have revealed the role of OPTN in regulating osteoblast function, which may be dominant over its role in osteoclasts. Although OPTN has been functionally analyzed concerning diseases in the fields of ophthalmology and neurology, in the present study, we have documented its role in bone metabolism, and further research can shed insight on its role in bone metabolic diseases.

Acknowledgments

We thank Editage (www. editage.jp) for English language editing, Ito Bone Science Institute for histomorphometric analysis, and Kureha Special Laboratory for immune histochemical analysis.

Competing Interests

The authors have no conflicts of interest to declare.

Disclosure

The authors report no disclosures regarding this manuscript.

Funding statement

This work was supported in part by the Japan Society for the Promotion of Science KAKENHI Grant-in-Aid for Scientific Research (No. 15K11388 and 18H0297800), a GSK Japan Research Grant from Glaxo Smith Kline, and the Takeda Science Foundation.

References

[1] T. Rezaie, A. Child, R. Hitchings, et al., Adult-onset primary open-angle glaucoma caused by mutations in optineurin, Science. 295 (2002) 1077–1079. https://doi.org/10.1126/science.1066901.

[2] H. Maruyama, H. Morino, H. Ito, et al., Mutations of optineurin in amyotrophic lateral sclerosis,

Nature. 465 (2010) 223–226.

[3] Z. L. Chi, M. Akahori, M. Obazawa, et al., Overexpression of optineurin E50K disrupts Rab8 interaction and leads to a progressive retinal degeneration in mice, Hum Mol Genet. 19 (13) (2010) 2606–2615. https://doi.org/10.1093/hmg/ddq146.

[4] D. A. Sahlender, R. C. Roberts, S. D. Ardenet al., Optineurin links myosin VI to the Golgi complex and is involved in Golgi organization and exocytosis, J Cell Biol. 169 (2005) 285–295. https://doi.org/10.1083/jcb.200501162.

[5] G. Zhu, C. J. Wu, Y. Zhao, et al., Optineurin negatively regulates TNFalpha- induced NF-kappaB activation by competing with NEMO for ubiquitinated RIP, Curr Biol. 17 (2007) 1438–1443. https://doi.org/10.1016/j.cub.2007.07.041.

[6] H. Ying, B. Y. Yue, Cellular and molecular biology of optineurin, Int Rev Cell Mol Biol. 294 (2012) 223–258.

[7] M. Akizuki, H. Yamashita, K. Uemura, et al., Optineurin suppression causes neuronal cell death via NF-κB pathway, J Neurochem. 126 (2013) 699–704. https://doi.org/10.1111/jnc.12326.

[8] P.Y.Chung, G. Beyens, S. Boonen, et al., The majority of the genetic risk for Paget's disease of bone is explained by genetic variants close to the CSF1, OPTN, TM7SF4, and TNFRSF11A genes, Hum Genet. 128 (2010) 615–626. https://doi.org/10.1007/s00439-010-0888-2.

[9] O. M. Albagha, S. E. Wani, M. R. Visconti, et al., Genome-wide association identifies three new

susceptibility loci for Paget's disease of bone, Nat Genet. 43 (2011) 685–689. https://doi.org/10.1038/ng.845.

[10] N. Laurin, J. P. Brown, J. Morissette, et al., Recurrent mutation of the gene encoding sequestosome 1 (SQSTM1/p62) in Paget disease of bone, Am J Hum Genet. 70 (2002) 1582–1588. https://doi.org/10.1086/340731.

[11] D. L. Galson, G. D. Roodman, Pathobiology of Paget's disease of bone, J Bone Metab. 21 (2014) 85–98. https://doi.org/10.11005/jbm.2014.21.2.85.

[12] R. Obaid, S. E. Wani, A. Azfer, et al., Optineurin negatively regulates osteoclast differentiation by modulating NF-κB and interferon signaling: Implications for Paget's disease. Cell Rep. 13 (2015) 1096–1102. https://doi.org/10.1016/j.celrep.2015.09.071

[13] A. Nagabhushana, M. Bansal, G. Swarup, 2011. Optineurin is required for CYLD-dependent inhibition of TNFα-induced NF-κB activation, PLoS One. 6, e17477. https://doi.org/10.1371/journal.pone.0017477.

[14] C. E. Gleason, A. Ordureau, R. Gourlay, et al., Polyubiquitin binding to optineurin is required for optimal activation of TANK-binding kinase 1 and production of interferon β, J Biol Chem. 286 (2011) 35663–35674. https://doi.org/10.1074/jbc.m111.267567.

[15] T. J. Martin, N. A. Sims, Osteoclast-derived activity in the coupling of bone formation to resorption, Trends Mol Med. 11 (2005) 76–81. https://doi.org/10.1016/j.molmed.2004.12.004.

[16] N. Leavaot, P. D. Simoncic, I. D. Dimitriou, et al., 3BP2-deficient mice are osteoporotic with impaired osteoblast and osteoclast functions, N. Levaot, J Clin Invest. 121 (2011) 3244–3257. https://doi.org/10.1172/jci45843.

[17] M. Hayashi, T. Nakashima, M. Taniguchi, et al., Osteoprotection by semaphorin 3A, Nature. 485 (2012) 69–74. https://doi.org/10.1038/nature11000.

[18] Y. Miyauchi, K. Ninomiya, H. Miyamoto, et al., The Blimp1-Bcl6 axis is critical to regulate osteoclast differentiation and bone homeostasis, J Exp Med. 207 (2010) 751–762. https://doi.org/10.1084/jem.20091957.

[19] A Fujie, A Funayama, Y Miyauchi, et al., Bcl6 promotes osteoblastogenesis through Stat1 inhibition, Biochem Biophys Res Commun. 457 (2013) 451–456. https://doi.org/10.1016/j.bbrc.2015.01.012.

[20] J. Lee, M. Kim, J. Byun, et al., The effect of biomechanical stimulation on osteoblast differentiation of human jaw periosteum-derived stem cells, Maxillofac Plast Reconstr Surg. 39 (2017) 7. https://doi.org/10.1186/s40902-017-0104-6.

[21] H. Kim, K. Iwasaki, T. Miyake et al., Changes in bone turnover markers during 14-day 6 head-down bed rest, J Bone Miner Metab. 21 (2003) 311–315. https://doi.org/10.1007/s00774-003-0426-6.

[22] M. M. Deckers, M. Karperien, C. van der Bent, et al., Expression of vascular endothelial growth factors and their receptors during osteoblast differentiation, Endocrinology. 141 (2000) 1667–1674. https://doi.org/10.1210/en.141.5.1667.

[23] S. Kim, T. Koga, M. Isobe, et al., Stat1 functions as a cytoplasmic attenuator of Runx2 in the transcriptional program of osteoblast differentiation, Genes Dev. 17 (16) (2003) 1979–1991. https://doi.org/10.1101/gad.1119303.

[24] S. Nakazawa, D. Oikawa, R. Ishii, Linear ubiquitination is involved in the pathogenesis of optineurin-associated amyotrophic lateral sclerosis, Nat Commun. 7 (2016) 12547. https://doi.org/10.1038/ncomms12547.

Figure Legends

Fig. 1.

The bone phenotype of Optn$^{-/-}$ mice. (A) Immunohistochemical detection of RUNX2. Black arrows indicate representative RUNX2 positive osteoblasts. Scale bar = 10 μm. (B-C) Graphs representing the comparison of (B) Obs/BS and (C) ObN/BS. Obs/BS, osteoblast surface per bone surface; ObN/BS, osteoblast number per bone surface. (D) Representative images of osteoid thickness. Scale bar = 10 μm. (E) Representative images of calcein-tetracyclin labeled femur. Scale bar = 10 μm. (F-G) Graphs representing the comparison of dynamic bone formation indices. (F)

MAR; mineral apposition rate, (G) BFR/BS; bone formation rate per bone surface. (H-J) Graphs representing the comparison of (H) Oth, (I) Omt, and (J) Mit. (Oth, osteoid thickness; Omt, osteoid maturation time; Mit, mineralization lag time). Values represent mean ± SD. *$p < 0.05$, **$p < 0.01$.

Fig. 2.

Inhibition of osteoblast differentiation by OPTN *in vitro*. (A) *In vitro* osteoblast maturation assay. Osteoblasts were cultured for 21 days and stained for ALP after 7, 14, or 21 days of culture. (B) Quantification of ALP activity after 7 and 14 days of culture. (C, D) Mineralized nodule formation as determined by Alizarin Red staining after 21 days of culture. Scale bar = 10 μm.

Fig. 3.

OPTN promotes osteoblastogenesis by STAT1 inhibition. (A) Binding of OPTN to STAT1 in osteoblasts. STAT1 was immunoprecipitated (IP) from cell lysates, and the presence of STAT1 and OPTN in the immunoprecipitates was analyzed by western blotting (WB). (B) WB of STAT1 protein levels in osteoblasts. (C) Immunofluorescent staining of nuclei and RUNX2 visualized by DAPI and anti-RUNX2 antibody, respectively. (D) Quantitation of RUNX2-positive nuclei. The percentage of RUNX2-positive nuclei per total nuclei was measured. Scale bar = 50 μm. Values represent mean ± SD. **$p < 0.01$.

Fig. 4.

Impaired osteoblast function in $Optn^{-/-}$ mice. (A) Osteoblast-osteoclast co-culture assay. The numbers of $TRAP^{+}$ MNCs were counted. Values represent mean ± SD. (B) Quantitative PCR of *tnfsf11* mRNA levels in osteoblasts. $*p < 0.05$, $**p < 0.01$.

Figure1

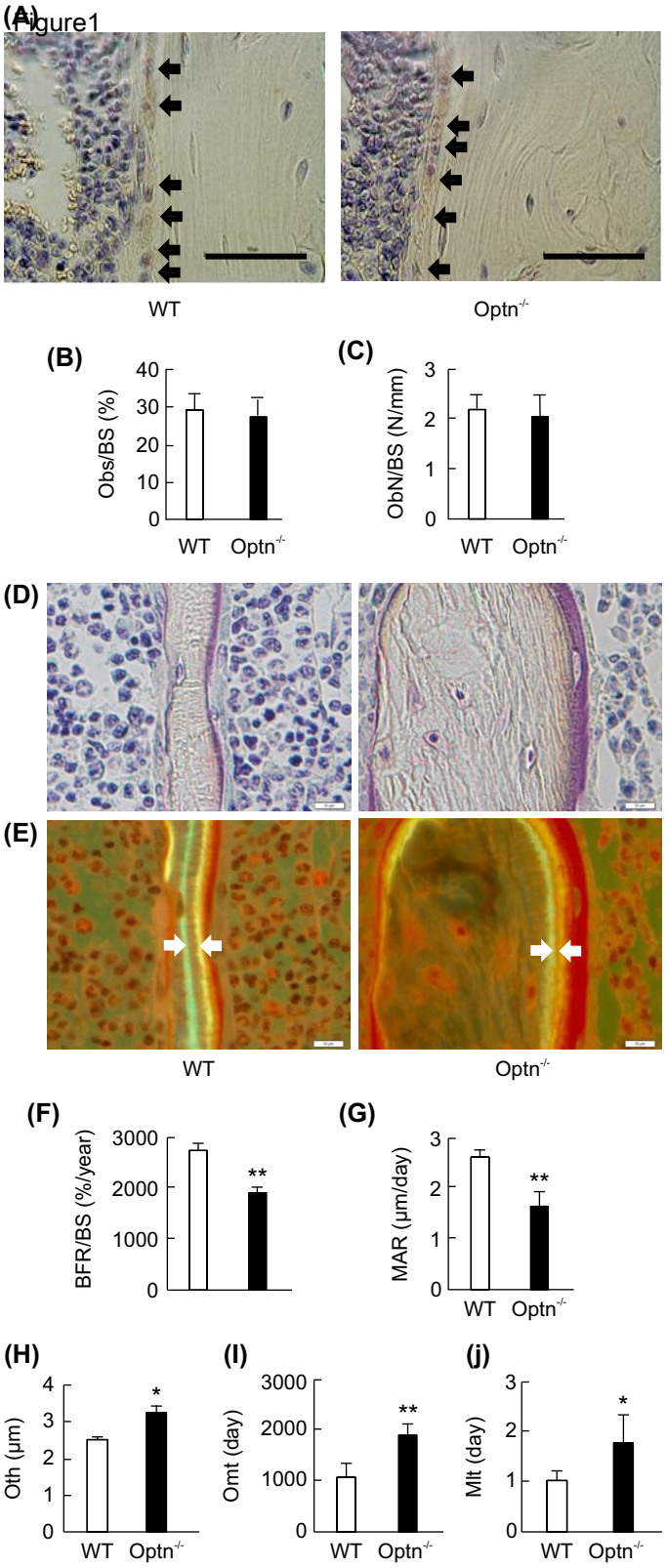
(A)
WT
Optn-/-
(B)
Obs/BS (%)
40
30
20
10
0
WT
Optn-/-
(C)
ObN/BS (N/mm)
3
2
1
0
WT
Optn-/-
(D)
(E)
WT
Optn-/-
(F)
BFR/BS (%/year)
3000
2000
1000
0
**
(G)
MAR (μm/day)
3
2
1
0
**
WT
Optn-/-
(H)
Oth (μm)
4
3
2
1
0
*
WT
Optn-/-
(I)
Omt (day)
3000
2000
1000
0
**
WT
Optn-/-
(j)
Mlt (day)
3
2
1
0
*
WT
Optn-/-

Figure2

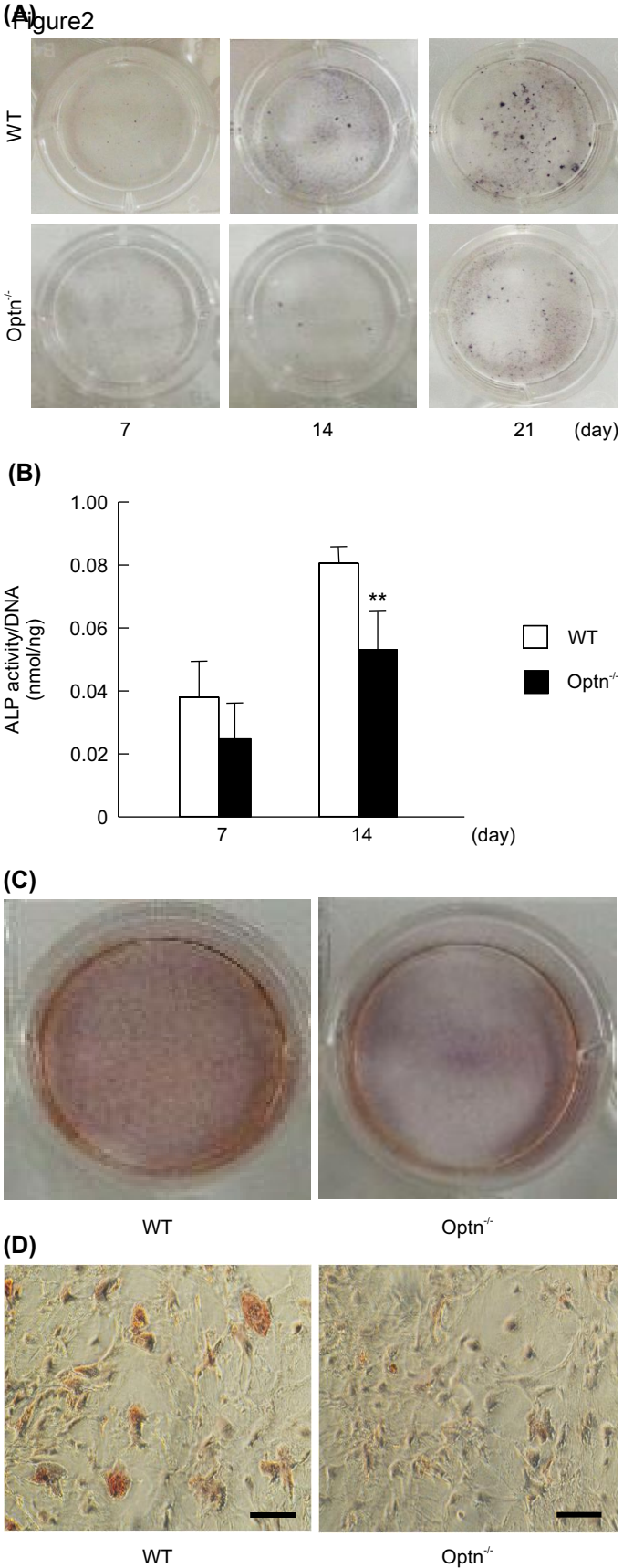
(A)
WT
Optn-/-
7
14
21
(day)
(B)
ALP activity/DNA (nmol/ng)
1.00
0.08
0.06
0.04
0.02
0
**
7
14
(day)
WT
Optn-/-
(C)
WT
Optn-/-
(D)
WT
Optn-/-

Figure3

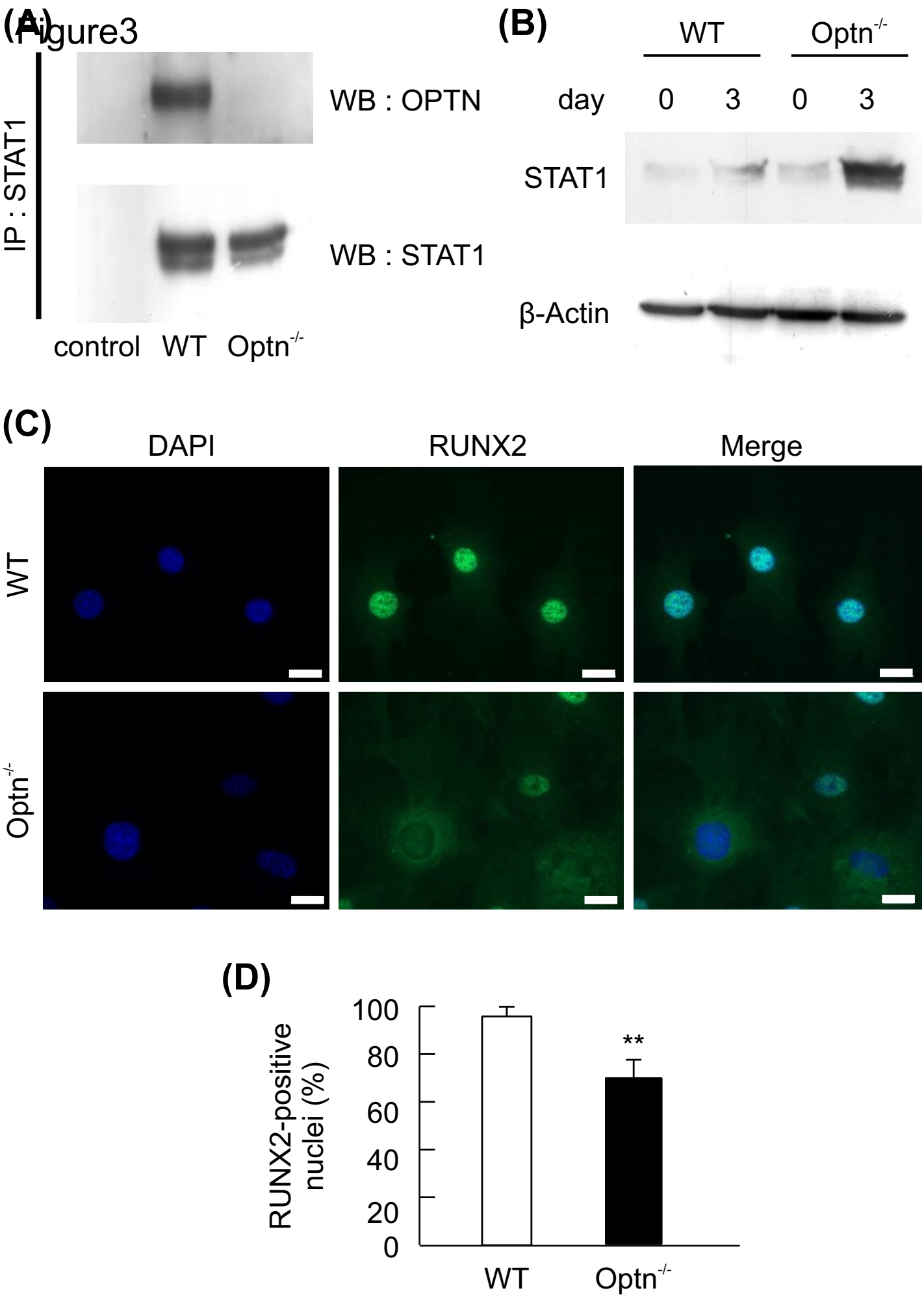
(A)
IP : STAT1
WB : OPTN
WB : STAT1
control
WT
Optn-/-
(B)
WT
Optn-/-
day
0
3
0
3
STAT1
β-Actin
(C)
DAPI
RUNX2
Merge
WT
Optn-/-
(D)
RUNX2-positive nuclei (%)
100
80
60
40
20
0
**
WT
Optn-/-

Figure4

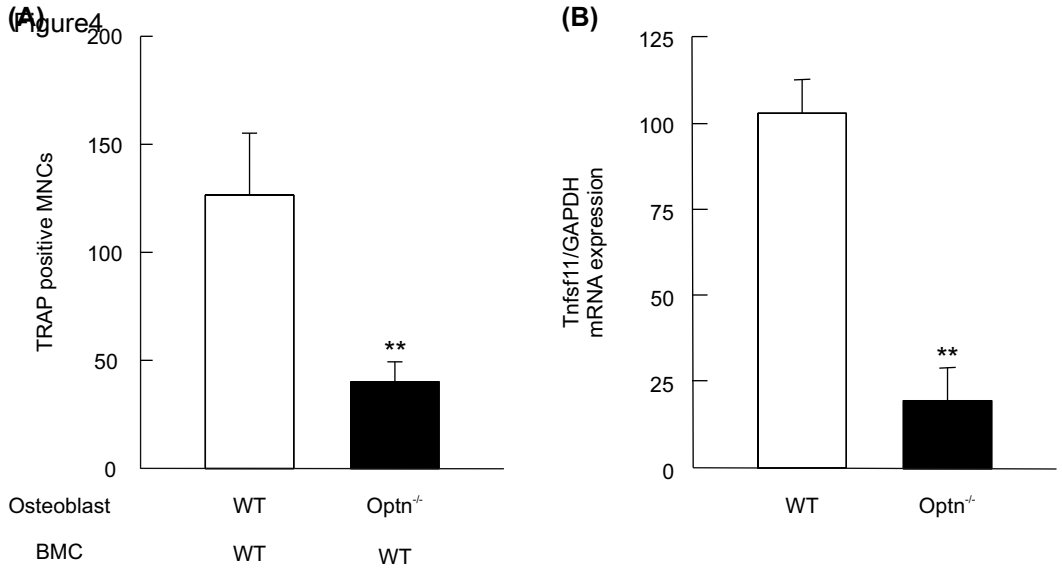
(A)
TRAP positive MNCs
200
150
100
50
0
**
Osteoblast
WT
Optn-/-
BMC
WT
WT
(B)
Tnfsf11/GAPDH
mRNA expression
125
100
75
50
25
0
**
WT
Optn-/-